

fractions are similar suggests that these fractions are all produced by the same catalyst. The fractionation results imply that the polymers are characterized by a distribution of block lengths for the isotactic and atactic stereosequences. This is consistent with a two-site propagation mechanism, as a distribution of block lengths would be expected for a kinetically controlled process.

Several polypropylene samples formed with the  $(2\text{-PhInd})_2\text{ZrCl}_2/\text{MAO}$  catalyst system were analyzed by differential scanning calorimetry. Sample PP4 exhibited peak melting points at 52.1° and 78.7°C. Samples with higher [mmmm] showed higher melting points: sample PP9 exhibited a broad melting transition between 125° and 145°C with a heat of fusion of 0.4 J g<sup>-1</sup>. The physical properties of PP4 revealed an initial modulus of 246 psi (17.3 kg cm<sup>-2</sup>), a tensile strength of 462 psi (32.5 kg cm<sup>-2</sup>), and an ultimate elongation of 1210%. The elastic properties were further demonstrated by hysteresis tests, where elongation to 300% resulted in a tensile set of 50%.

## REFERENCES AND NOTES

- Thermoplastic elastomers are polymers that exhibit elastic properties yet soften and flow upon heating, unlike conventional vulcanized rubbers.
- G. Natta, G. Mazzanti, G. Crespi, G. Moraglio, *Chim. Ind. Milan* **39**, 275 (1957); G. Natta, *J. Polym. Sci.* **34**, 531 (1959); \_\_\_\_\_ and G. Crespi, U.S. Patent 3,175,999 (1965).
- J. W. Collette and C. W. Tullock, U.S. Patent 4,335,225 (1982); J. W. Collette *et al.*, *Macromolecules* **22**, 3851 (1989); J. W. Collette, D. W. Ovenall, W. H. Buck, R. C. Ferguson, *ibid.*, p. 3858.
- D. T. Mallin, M. D. Rausch, Y. G. Lin, S. Dong, J. C. W. Chien, *J. Am. Chem. Soc.* **112**, 2030 (1990); J. C. W. Chien *et al.*, *ibid.* **113**, 8569 (1991).
- F. R. W. P. Wild, L. Zsolnai, G. Huttner, H. H. Brintzinger, *J. Organomet. Chem.* **232**, 233 (1982).
- J. A. Ewen, *J. Am. Chem. Soc.* **106**, 6355 (1984).
- W. Kaminsky, K. Kùlper, H. H. Brintzinger, F. R. W. P. Wild, *Angew. Chem. Int. Ed. Engl.* **24**, 507 (1985).
- See also G. Erker *et al.*, *J. Am. Chem. Soc.* **115**, 4590 (1993).
- B. D. Coleman and T. G. Fox, *J. Chem. Phys.* **38**, 1065 (1963).
- 2-Phenylindene was prepared in 64% yield by the addition of 2-indanone to phenylmagnesium bromide, followed by dehydration with *p*-toluenesulfonic acid. Deprotonation of 2-phenylindene with butyllithium yielded 2-phenylindenyllithium, which was used without further purification.
- A.-L. Mogstad, M. D. Bruce, R. M. Waymouth, unpublished material; W. D. Luke and A. Streitwieser, *J. Am. Chem. Soc.* **103**, 3241 (1981); J. Okuda, *J. Organomet. Chem.* **356**, C43 (1988).
- C. Krüger, M. Nolte, G. Erker, S. Thiele, *Z. Naturforsch. Teil B* **47**, 995 (1992).
- X-ray structure analysis of  $(2\text{-PhInd})_2\text{ZrCl}_2$ : space group  $P\bar{1}$  (no. 2), unit cell constants  $a = 13.538(2)$  Å,  $b = 14.553(2)$  Å,  $c = 15.365(1)$  Å,  $\alpha = 65.78(1)^\circ$ ,  $\beta = 64.95(1)^\circ$ ,  $\gamma = 63.16(1)^\circ$ ,  $V$  (unit cell volume) = 2355.4(6) Å<sup>3</sup>,  $d_{\text{calc}}$  (density) = 1.54 g cm<sup>-3</sup>,  $\mu_{\text{calc}}$  (absorption coefficient) = 7.1 cm<sup>-1</sup>,  $Z$  (molecules per unit cell) = 4 (numbers in parentheses are the standard errors in the last digit). Total number of reflections = 8658, reflections with  $[F_o^2 > 3\sigma(F_o^2)] = 6362$ , where  $F_o$  is the structure factor,  $R = 0.032$ ,  $R_w = 0.032$ . During refinement, a slight disordering of the *syn* rotamer was revealed, requiring refinement at 96% occupancy. Selected bond lengths (in angstroms) for the crystallographically independent rotamers: Zr(1)-Cl(1) 2.4267(9), Zr(2)-Cl(3) 2.4334(9), Zr(1)-Cl(2) 2.421(1), Zr(2)-Cl(4) 2.421(2), Zr(1)-Cl(1) 2.482(5), Zr(2)-Cl(3) 2.476(4), Zr(1)-Cl(2) 2.561(3), Zr(2)-Cl(3) 2.504(4), Zr(1)-Cl(3) 2.558(3), Zr(2)-Cl(3) 2.523(3), Zr(1)-Cl(4) 2.612(4), Zr(2)-Cl(3) 2.624(3), Zr(1)-Cl(9) 2.531(5), Zr(2)-Cl(3) 2.570(3), Zr(1)-Cl(16) 2.465(3), Zr(2)-Cl(4) 2.485(5), Zr(1)-Cl(17) 2.551(3), Zr(2)-Cl(4) 2.553(4), Zr(1)-Cl(18) 2.564(3), Zr(2)-Cl(4) 2.529(3), Zr(1)-Cl(19) 2.622(3), Zr(2)-Cl(4) 2.591(3), Zr(1)-Cl(24) 2.527(3), Zr(2)-Cl(5) 2.559(4). Selected angles for the crystallographically independent rotamers (in degrees): Cl(1)-Zr(1)-Cl(2) 95.44(4), Cl(3)-Zr(2)-Cl(4) 94.39(4), Cl(2)-Cl(1)-Cl(9) 107.3(3), Cl(3)-Cl(3)-Cl(3) 109.1(4), Cl(1)-Cl(2)-Cl(3) 108.0(3), Cl(3)-Cl(3)-Cl(3) 106.6(4), Cl(2)-Cl(3)-Cl(4) 108.4(4), Cl(3)-Cl(3)-Cl(3) 109.4(3), Cl(3)-Cl(4)-Cl(9) 107.8(3), Cl(3)-Cl(3)-Cl(3) 107.2(4), Cl(1)-Cl(9)-Cl(4) 108.2(4), Cl(3)-Cl(3)-Cl(3) 107.5(3), Cl(17)-Cl(16)-Cl(24) 108.2(4), Cl(47)-Cl(46)-Cl(54) 108.4(4), Cl(16)-Cl(17)-Cl(18) 107.2(3), Cl(46)-Cl(47)-Cl(48) 108.1(3), Cl(17)-Cl(18)-Cl(19) 108.8(3), Cl(47)-Cl(48)-Cl(49) 108.4(4), Cl(18)-Cl(19)-Cl(24) 107.3(4), Cl(48)-Cl(49)-Cl(54) 107.0(4), Cl(16)-Cl(24)-Cl(19) 108.2(3), Cl(46)-Cl(54)-Cl(49) 107.6(3), Ce-Zr(1)-Ce 131.3, Ce-Zr(2)-Ce 131.0 (Ce is the centroid of the five-membered ring).
- C. Krüger, F. Lutz, M. Nolte, G. Erker, M. Aulbach, *J. Organomet. Chem.* **452**, 79 (1993). For an example of a related structure,  $\text{K}[\text{Ti}(\eta^6\text{-biphenyl})_2]$ , which exhibits *syn* and *anti* rotamers, see D. W. Blackburn, D. Britton, J. E. Ellis, *Angew. Chem. Int. Ed. Engl.* **31**, 1495 (1992).
- A. Grassi, A. Zambelli, L. Resconi, E. Albizzati, R. Mazzocchi, *Macromolecules* **21**, 617 (1988); P. Corradini, V. Busico, R. Cipullo, *Makromol. Chem. Rapid Commun.* **13**, 21 (1992).
- W. Spaleck *et al.*, *Angew. Chem. Int. Ed. Engl.* **31**, 1347 (1992).
- Two neighboring stereocenters are described as meso (m) if they are of the same relative stereochemistry and racemic (r) if they are of opposite stereochemistry.
- J. A. Ewen *et al.*, *Stud. Surface Sci. Catal.* **56**, 439 (1990); B. Rieger, G. Jany, R. Fawzi, M. Steimann, *Organometallics* **13**, 647 (1994); V. Busico, R. Cipullo, *J. Am. Chem. Soc.* **116**, 9329 (1994).
- F. A. Bovey, *High Resolution NMR of Macromolecules* (Academic Press, New York, 1972).
- A. Zambelli, P. Locatelli, A. Provasoli, D. R. Ferro, *Macromolecules* **13**, 267 (1980).
- S.-N. Zhu, X.-Z. Yang, R. Chùjò, *Polym. J.* **15**, 859 (1983); Y. Inoue, Y. Itabashi, R. Chùjò, Y. Doi, *Polymer* **25**, 1640 (1984).
- A.-L. Mogstad, thesis, Stanford University (1994).
- We thank E. Moore and A. Ernst for the mechanical analysis of polymer samples, A.-L. Mogstad for carrying out polymer fractionation studies, and T. D. P. Stack for obtaining the x-ray crystal structure. We are grateful to Amoco and the National Science Foundation (grant DMR-9258324) for financial support. R.M.W. acknowledges the A. P. Sloan Foundation for a fellowship and the National Science Foundation for a National Young Investigator award, and G.W.C. acknowledges the Hertz Foundation for a fellowship.

22 August 1994; accepted 15 November 1994

## Segregation in DNA Solutions Induced by Electric Fields

L. Mitnik, C. Heller, J. Prost, J. L. Viovy\*

DNA solutions subjected to an electric field exhibit an instability that leads to DNA segregation in aggregates tilted with regard to the field. With the use of epifluorescence videomicroscopy, the evolution of DNA patterns in capillaries as a function of DNA concentration, DNA size, field strength, and field frequency was studied. The field threshold for segregation was decreased when the frequency was lowered or when the DNA molecular weight or concentration was increased. Aggregation is attributed to an electrohydrodynamic instability triggered by the dipole-dipole interaction. This phenomenon explains the failure of earlier attempts to separate large DNA in capillaries.

Molecular genetics relies heavily on the electrophoretic separation of DNA molecules by size. Until recently, this was achieved mainly in slab gels, but the joint use of capillary electrophoresis (CE) and liquid sieving media (solutions of hydrophilic polymers) has gained increasing popularity (1). The performances of CE for DNA fragments up to a few kilobases are excellent. Attempts to separate larger fragments have failed, however, and electrophoregrams containing many unexplained and irreproducible peaks were obtained (2, 3). To investigate this question, we developed a microcapillary electrophoresis sys-

tem in which the behavior of solutions containing fluorescently labeled DNA can be directly observed by intensified videomicroscopy (Fig. 1).

The first experiments were performed under a continuous field in a sieving buffer similar to those used in CE—that is, 1× TBE (89 mM tris-boric acid and 2.5 mM EDTA), 0.2% w/w hydroxypropyl cellulose (HPC; 10<sup>6</sup> molecular weight; Sigma), and 10 μM ethidium bromide for fluorescent labeling (4). Three monodisperse duplex DNA samples (bacteriophage T4, 166 kilobase pairs, Amersham, United Kingdom; bacteriophage λ, 48.5 kilobase pairs, Appligene, Illkirch F; and pBR 322, 4361 base pairs, BioLabs, Beverly, Massachusetts) were used at concentrations ranging from 0.05 to 75 μg/ml. For pBR 322, the highest concentration we studied was 25 μg/ml, and no segregation was observed in the frequen-

Laboratoire de Physicochimie théorique (Unité Associée au CNRS 1382) et Laboratoire de Physicochimie Structurale et Macromoléculaire (Unité Associée au CNRS 278), ESPCI, 10 rue Vauquelin, 75231 Paris Cedex 05, France.

\*To whom correspondence should be addressed.

cy and field strength range studied. For T4 and  $\lambda$  DNA, strong density fluctuations appeared at high concentrations and electric fields above a few tens of volts per centimeter (V/cm). Concentrated regions developed, moved, and deformed in a complicated manner, making a quantitative study difficult. We then subjected DNA solutions to square pulsed electric fields, over a frequency range of  $10^{-2}$  to  $10^5$  Hz and a field strength range of 10 to 100 V/cm. At the low end of the frequency range, the behavior is essentially the same as in a constant field. We also lowered the HPC concentration to  $10^{-4}$  w/w, much below its overlap concentration of about  $1.5 \times 10^{-3}$  w/w. The electrophoretic mobility varied, but the threshold for segregation and the patterns appeared to depend only weakly on HPC concentration. We conclude that DNA segregation is not due to the viscoelastic behavior of the buffer. With no HPC added, however, the pattern of aggregates at low frequencies is strongly modified. We attribute this to electroosmosis, because HPC, which adsorbs strongly on glass surfaces, is an efficient suppressor of electroosmosis even at very low concentrations; this was demonstrated by the strongly reduced mobility of neutral dyes in conventional CE (5).

In the short square capillaries used in microscopy experiments, we were obliged to seal both ends of the capillary with agarose to prevent spurious flow that was a result of gravity and capillary forces. In such a case, electroosmosis leads to a buffer recirculation in the center of the capillary having a Poiseuille profile with nonzero mobility at the wall (in contrast to open capillaries in which the electroosmotic profile is pluglike). We confirmed the suppression of electroosmosis by HPC in our experiments by measuring the profile of the longitudinal velocity of 0.4- $\mu$ m-diameter latex beads (Molecular Probes, Eugene, Oregon). In the presence of 0.01% HPC, the profile was pluglike within experimental error, whereas in the absence of HPC it was essentially Poiseuille-like with an offset. The buffer recirculation is able to interfere with the formation of aggregates, so in all subsequent experiments 0.01% HPC was added to the solutions. The hypothesis that the instability leading to DNA aggregation could be a result of residual electroosmosis and not DNA was ruled out, because solutions containing very minute amounts of DNA (0.04  $\mu$ g/ml) or latex as tracers presented no instability in the range of field strength studied.

The peak-to-peak voltage threshold for the appearance of segregation is plotted in Fig. 2: high field strengths, low frequencies, large DNA size, and high DNA concentration all tend to favor segregation. Segregation can occur much below the overlap

concentration of DNA molecules (6). We studied in particular detail the evolution of concentration patterns at 20 Hz: at this frequency, the segregation effect was strong, but the DNA motion during one half-period was smaller than the size of the smallest visible aggregates (typically a few micrometers), so that direct electrophoretic motion was negligible. The early stage patterns seemed rather independent of field strength and capillary size, but their rate of evolution depended strongly on the field strength.

A typical series of patterns obtained after application of the electric field for 2 min is given in Fig. 3, A through F, for several field strengths (the evolution for increasing field strength closely resembles the time sequence of patterns at a high fixed field strength). At first, the solution separated into tortuous domains roughly resembling a spinodal decomposition, but presenting in addition a privileged tilt angle of about  $60^\circ$  to  $70^\circ$  with respect to the field. These domains progressively rearranged to form pluglike or disklike aggregates the size of the capillary. The distance between the domains was somewhat larger than the capillary section (see Fig. 3, F through H). It tended to increase slowly at long times, when pairs of aggregates collapsed from time to time to yield a larger one. The dynamic video observations showed that the aggregates tumbled slowly and remained tilted in average. This privileged orientation was confirmed by a similar experiment performed in a slab cell, which yielded irregular chevronlike stripes with a similar angle of tilt. The dynamic observation of individual  $\lambda$  DNA molecules at very low concentration (0.04  $\mu$ g/ml), labeled with YOYO (Molecular Probes) and dissolved in a more concentrated (30  $\mu$ g/ml) matrix of unlabeled ones, showed that individual molecules are permanently recirculated inside each aggregate. The concentration inside the aggregates (qualitatively reflected by the brightness) increased with increasing field strength, and the thickness of the aggregates decreased at the same time. At a given field strength, more dilute DNA solutions yielded thinner aggregates. From these observations, we infer that the electric field induces an attractive force between DNA molecules or aggregates, up to some concentration that increases with the field.

In colloid physics, it has been known for a long time that an alternating field can induce the aggregation of polarizable particles (such as latex beads) by an induced dipole-dipole attraction. In general, particles align in the direction of the field (7), in contrast with the behavior we observed for DNA. Very recently, however, Hu *et al.* reported the formation of tilted aggregates with particle recirculation in concentrated

suspensions of polystyrene spheres subjected to alternating fields of the order of 800 V/cm, with frequencies in the range of 100 kHz (8). They attributed this unusual behavior to a rather subtle instability mechanism: because of the retardation of the induced dipole, neighboring particles with a center-to-center vector tilted with regard to the field rotated and exerted on each other a hydrodynamic force that tended to increase the angle of tilt. A complete theory of this phenomenon is not yet available, but Hu *et al.* confirmed by computer simulations that the proposed mechanism is able to generate tilted aggregates with internal recirculation.

We believe that the aggregation we observed for DNA in alternating fields has the same physical origin. Because DNA solutions present a huge polarizability at low

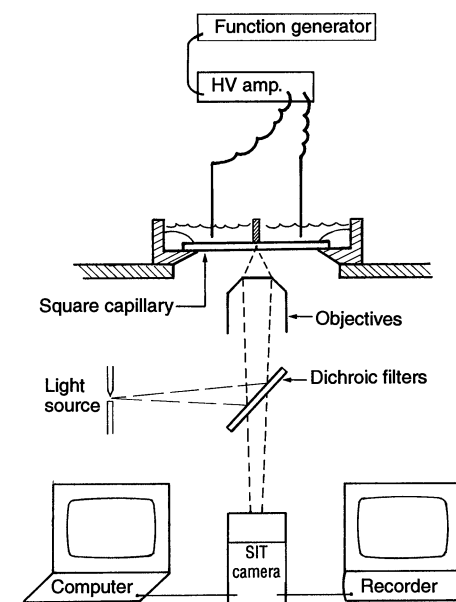


**Fig. 1.** Several 25-mm-long microbore tubes with a square internal section ( $50 \mu\text{m}$  by  $50 \mu\text{m}$ ,  $100 \mu\text{m}$  by  $100 \mu\text{m}$ , and  $200 \mu\text{m}$  by  $200 \mu\text{m}$ ; Vitro-Dynamics, Rockaway, New Jersey) were placed on an annular polycarbonate sheet, then covered with a disklike cover slide and placed in a two-compartment cylindrical chamber with platinum electrodes. Sealings were performed with silicone grease. The tubes were filled by capillarity with the appropriate solutions and immediately sealed with low-melt agarose (Seaprep FMC) prepared with the same buffer. The chamber was placed in a Zeiss Axiovert 135 TV inverted microscope. Objectives with magnifications ranging from  $5\times$  to  $100\times$  were used, depending on experimental conditions. Images were either collected by a SIT camera (LHESA Electronics, Cergy, France) and recorded on VHS or photographed on high-sensitivity 35-mm film. Pulsed or continuous electric fields were generated by a 0- to 1-MHz amplifier (HV amp.) (Krohn-Hite, Avon, Massachusetts) driven by a programmable function generator (Hameg 8130, Francaise d'instrumentation, Troyes, France).

frequencies (which arises from the transport of counterions in the Debye layer), however, they can undergo segregation at lower field strengths than suspensions of latex beads. This interpretation is qualitatively consistent with our main experimental observations. There is a voltage threshold for aggregation because the osmotic pressure of counterions must be overcome by the electrohydrodynamic instability. When the field is switched off, the aggregates progressively spread out and a homogeneous solution is recovered by diffusion after a few hours. The threshold for aggregation strongly depends on the frequency in the range of 0.1 Hz to 1 kHz, which corresponds to a dispersion range of the ionic polarizability of DNA molecules in the range of 10 to 100 kb (9). In this dispersion range, the retardation of the induced dipoles should be strong, and the instability mechanism proposed by Hu *et al.* (8) is very plausible. The threshold also depends on DNA size (as the polarizability) and on the concentration (as the strength of dipolar and hydrodynamic couplings between molecules). Finally, DNA molecules recirculate inside the aggregates, as observed for latex beads (8).

In constant fields, we also observed aggregation as Song and Maestre did in an earlier study (10): these authors reported that very dilute DNA solutions aggregated in "snowballs" when submitted to constant fields above 400 V/cm (that is, typically 10

times larger than the ones used in our experiments). They attributed this aggregation to entanglements occurring during successive collisions between DNA molecules in the course of migration, analogous to a well-known behavior in sedimentation. Entanglements may play a role in the late stages of aggregation, but we believe that the electrophoretic force alone cannot induce aggregation: it drives all DNA molecules at the same velocity (in contrast to sedimentation, for example), and the entropy of counterions should keep them apart. Another interaction, attractive, is necessary to explain the observed aggregation.

Also, collisions induced by electrophoresis cannot explain why we observed aggregation in alternating fields at frequencies as high as 1 kHz, at which the electrophoretic motion of one molecule during one half-period is smaller than its radius of gyration at rest, or the recirculation of molecules inside one aggregate on distances of several hundred microns. We believe that the induced dipole-dipole interaction, rather than

the collisions, is the primary driving force for aggregation in constant fields as in alternating fields. In constant fields, however, the description proposed above is no longer sufficient, because there is no retardation of the induced dipole and because of additional hydrodynamic interactions between aggregates arising from the electrophoretic drift, which can be coupled to DNA concentration. In particular, we observed that large aggregates formed in a constant field tend to avoid each other in the course of migration; this suggests that hydrodynamic interactions are not screened. This fact, in contrast with the common view that polyelectrolytes are free-draining in the high-salt limit (11), warrants further investigation.

The field strength conditions in which we observed segregation are typical of those encountered in earlier dielectric or electrooptic studies of DNA solutions (9). Therefore, one should wonder if some properties earlier attributed to individual DNA molecules were not connected in part with the collective behavior reported

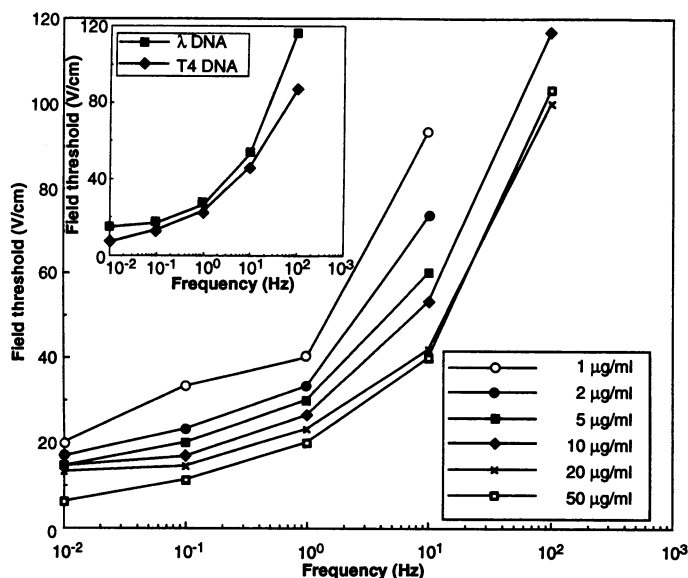
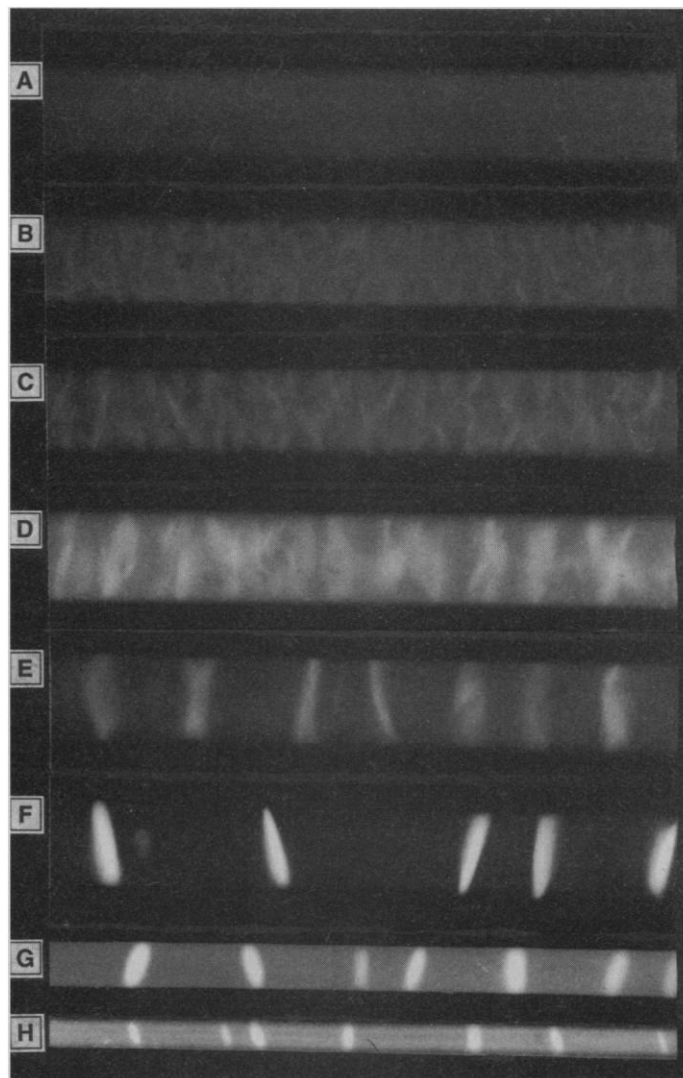


**Fig. 2 (left).** Evolution of the field threshold for segregation versus frequency for  $\lambda$  DNA. Inset: comparison of the threshold for T4 and  $\lambda$  DNA at 10  $\mu\text{g/ml}$ , with the use of a 0.2 mm by 0.2 mm by 25 mm cell. The uncertainty in the determination of the threshold, evaluated by repeated experiments, is 10%. **Fig. 3 (right).** Patterns of a  $\lambda$  DNA solution, 20  $\mu\text{g/ml}$ , in a 1  $\times$  TBE buffer containing 0.01% HPC and 10  $\mu\text{M}$  ethidium bromide. Square capillary, 200  $\mu\text{m}$  by 200  $\mu\text{m}$ ; frequency, 20 Hz; field strength, 0, 32, 40, 48, 60, and 80 V/cm [(A), (B), (C), (D), (E), and (F), respectively]. The patterns obtained in smaller capillaries are shown in (G) for a capillary 100  $\mu\text{m}$  by 100  $\mu\text{m}$  and in (H) for a capillary 50  $\mu\text{m}$  by 50  $\mu\text{m}$ .



here. Also, the fields we used are typical of those encountered in CE, and the electrokinetic preconcentration occurring at the entrance of the sieving polymer can lead to high DNA concentrations. We observed that aggregation can occur in a polymer-containing sieving buffer as well as in free solution, if large DNA molecules are present. Thus, aggregation can explain why electrophoregrams present numerous irreproducible peaks (1, 2), because each aggregate passing the detector yields a spurious peak. Understanding how aggregation occurs will be necessary to eliminate or reduce its occurrence and to extend the range of sizes and field strengths presently available for electrophoretic separations in liquid solutions.

## REFERENCES AND NOTES

1. P. D. Grossman and J. C. Colburn, Eds., *Capillary Electrophoresis: Theory and Practice* (Academic Press, San Diego, 1992).
2. S. Hjerten, T. Srichaiyo, K. Elenbring, paper presented at High Performance Capillary Electrophoresis

- '91, San Diego, CA, 3 to 6 February 1991.
3. T. Guszczynski, H. Pulayeva, T. Tietz, M. Garner, A. Chrambach, *Electrophoresis* **14**, 523 (1993).
4. Other concentrations of ethidium bromide were used without qualitative effects on the results.
5. See, for example, (1), p. 313.
6. The overlap concentration for T4 and  $\lambda$  DNA is 48 and 86  $\mu\text{g/ml}$ , respectively, evaluated with a persistence length of 500 Å and the Kratky-Porod formula. [O. Kratky and G. Porod, *Recl. Trav. Chim.* **68**, 1106 (1949)].
7. H. A. Pohl, *Dielectrophoresis* (Cambridge Univ. Press, Cambridge, UK, 1978), p. 135.
8. Y. Hu, J. L. Glass, A. E. Griffith, *J. Chem. Phys.* **100**, 4674 (1994).
9. See, for example, M. Jonsson, U. Jacobson, M. Takahashi, B. Norden, *J. Chem. Soc. Faraday Trans.* **89**, 2791 (1993); Z. Wang, R. Xu, B. Chu, *Macromolecules* **23**, 790 (1990). This may also explain why the dielectric constant of DNA solutions is difficult to measure below  $10^4$  Hz [M. Mandel, *Ann. N.Y. Acad. Sci.* **303**, 74 (1977)].
10. L. Song and M. F. Maestre, *J. Biomol. Struct. Dyn.* **9**, 525 (1991).
11. F. Brochard-Wyart and P. G. de Gennes, *C. R. Acad. Sci. Paris Ser. II* **307**, 1497 (1988).
12. This work was supported by European Community grant 930018 of the Human Genome program. We are indebted to A. Ajdari, H. Isambert, P. Lammert, L. Leibler, M. Rubinstein, G. Weill, and B. Zimm for stimulating discussions and comments.

3 August 1994; accepted 1 November 1994

# High-Rate, Gas-Phase Growth of MoS<sub>2</sub> Nested Inorganic Fullerenes and Nanotubes

Y. Feldman, E. Wasserman, D. J. Srolovitz, R. Tenne\*

The gas-phase reaction between MoO<sub>3-x</sub> and H<sub>2</sub>S in a reducing atmosphere at elevated temperatures (800° to 950°C) has been used to synthesize large quantities of an almost pure nested inorganic fullerene (IF) phase of MoS<sub>2</sub>. A uniform IF phase with a relatively narrow size distribution was obtained. The synthesis of IFs appears to require, in addition to careful control over the growth conditions, a specific turbulent flow regime. The x-ray spectra of the different samples show that, as the average size of the IF decreases, the van der Waals gap along the c axis increases, largely because of the strain involved in folding of the lamella. Large quantities of quite uniform nanotubes were obtained under modified preparation conditions.

Although graphite is the most stable form of carbon under ambient conditions, graphite nanoclusters have been shown to be unstable against folding and to close into fullerenes (1), nested fullerenes (NFs) (2), and nanotubes (3). It is believed (4) that the main stimulus to form carbon fullerenes (CFs) emanates from the large energy associated with the dangling covalent bonds of the peripheral carbon atoms in graphite nanoclusters. Recent theoretic-

cal work (5) suggests that multilayer NFs are thermodynamically more stable than single layer fullerenes that have the same number of carbon atoms. Although the growth conditions in most cases are far from equilibrium, some evidence in support of this theoretical work was obtained by careful annealing of amorphous carbon soot with the beam of a transmission electron microscope (TEM) (6).

Nanoclusters of layered metal dichalcogenide materials, such as WS<sub>2</sub>, were also recently shown (7-9) to be unstable against folding and to close on themselves to form NF-like structures (also designated IFs) and nanotubes, which are similar to their carbon predecessors. Although the driving force in this case is not likely to be very different, the detailed structure of the IFs is quite different from that of the CFs, largely

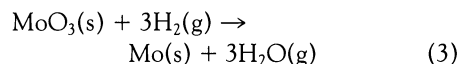
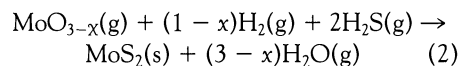
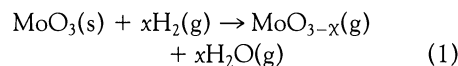
because the structures of graphite and layered dichalcogenides are different. In particular, the IFs are generally more faceted than the CFs (8, 9). In both the CFs and IFs, these folded, three-dimensional fullerenes are characterized by topological point defects on the basal planes of the regular crystal structure (10). However, the topological defects are much stronger in the IF structures than in the CF structures.

Because CFs can be considered a metastable form of carbon, it was suggested (11) that the ideal growth conditions for CFs could be provided through a gas-phase reaction. In this case, each nanocluster is isolated in the reaction chamber, and the only means for it to release its extra energy is through collisions with the noble carrier gas (He in most experiments). Development of a similar strategy for the IFs would be desirable but requires careful consideration and detailed knowledge of the phase equilibria in the reaction chamber.

However, the choice of source materials for a gas-phase reaction is fairly extensive. For example, preparation of MoS<sub>2</sub> powders and films by the gas-phase reaction between MoCl<sub>x</sub> (x = 3 to 5) and H<sub>2</sub>S (12) or MoF<sub>6</sub> and H<sub>2</sub>S (13) has been demonstrated. Alternatively, pulsed laser evaporation (14) and metal organic chemical vapor deposition (15) can be used to form IF from the gas phase.

To take advantage of the sublimation of MoO<sub>3-x</sub> at relatively low temperatures (>650°C), we built a reactor that allowed for a gas-phase reaction between a stream of gaseous molybdenum suboxide and H<sub>2</sub>S. This reactor was used to prepare, reproducibly, a few milligrams of an almost pure IF phase in each run. The production of copious amounts of IFs allowed a systematic study of the properties of the IF, the initial results of which are also reported here. Furthermore, the analysis of the growth conditions provided some clues to the pathway of IF production. Minor changes in the reactor design resulted in the production of substantial numbers of nanotubes up to 5  $\mu\text{m}$  in length with diameters of 10 to 20 nm.

To form MoS<sub>2</sub> from H<sub>2</sub>S and MoO<sub>3</sub> in a reducing atmosphere at elevated temperatures, the Mo-S-O ternary phase diagram should be considered (16) (see the schematic in Fig. 1). The following reactions are relevant for the growth of MoS<sub>2</sub> (represented by arrows in the phase diagram):



Y. Feldman and R. Tenne, Department of Materials and Interfaces, Weizmann Institute, Rehovot 76100, Israel. E. Wasserman, Central Research and Development Laboratories, E. I. du Pont de Nemours, Experimental Station, Wilmington, DE 19898, USA.

D. J. Srolovitz, Department of Materials and Interfaces, Weizmann Institute, Rehovot 76100, Israel, and Department of Materials Science and Engineering, University of Michigan, Ann Arbor, MI 48109, USA.

\*To whom correspondence should be addressed.